Experimental and Numerical Investigation of the Discharge Valve Limiter Geometric Features Change on Compressor Thermal Efficiency



A. Ekemen, A. Pinarbasi, C. Sahin, and A. Yildirim

Abstract The incorporation of inverter technology into hermetic reciprocating compressors has led to a significant decrease in energy consumption. However, to ensure efficient operation of the compressor components at varying rotation speeds, new optimizations are required. Discharge valves are one of the components most affected by high and low rotational speeds. Since the opening forces on the valves are high at high rotational speeds, they open and close properly, while flutter movements occur at lower rotational speeds. These flutter movements increase the discharge losses. Therefore, the movements of the discharge valves and the geometric features of the limiter, which restricts valve movement, play crucial roles in determining the discharge line losses and overall compressor efficiency. Variables such as the forces acting on the valve and the mass flow area are closely related with the maximum displacement of the discharge valve limited by the limiter. This study aims to prevent flutter movements and increase hermetic reciprocating compressor used in refrigerators efficiency by modifying the limiter geometric features. The results in working conditions of different condensation and evaporation temperatures at different rotation speeds, which were examined experimentally and numerically, are shared. Additionally, by utilizing a 1-D model solver, the compressor's efficiency is analyzed parametrically. The results indicate that reducing the limiter distance yields better outcomes at low rotation speeds in the higher compression ratio condition compared to lower compression ratio conditions and higher rotation speeds.

Keywords Reciprocating compressor · Discharge valves · Limiter · P–V diagrams · Valve displacement

A. Ekemen (✉) · C. Sahin · A. Yildirim
Arcelik A.Ş. Central R&D, Istanbul, Turkey
e-mail: alperen.ekemen@arcelik.com

A. Ekemen · A. Pinarbasi
Yildiz Technical University, Istanbul, Turkey

© The Author(s), under exclusive license to Springer Nature Switzerland AG 2024

M. Read et al. (eds.), *13th International Conference on Compressors and Their Systems*, Springer Proceedings in Energy, https://doi.org/10.1007/978-3-031-42663-6_36

1 Introduction

The introduction of inverter technology presents challenges in optimizing the performance of compressor components, particularly the valves. When making design changes that impact valve movements, the compressor efficiency can be influenced differently at various compression ratios. The exhaust time per cycle varies with the change in compression ratio, which leads to different results on valve movements.

The optimal operation of the exhaust valves involves their direct opening at the start of the exhaust phase, maintaining them open without any flutter until the end of the exhaust, and closing when the crank reaches the top dead point to prevent backflow. Flutter movements in the valves, particularly at low speeds, result in increased pressure within the cylinder and lead to additional energy consumption, thereby negatively impacting efficiency. To mitigate these flutters, optimization of valve stiffness and limiter distance is necessary. Extensive studies have been conducted in the literature concerning exhaust valves. For instance, Ichihara et al. [1] conducted experiments using valves of varying thicknesses and rotation speeds. Their findings demonstrated that thinner valves tend to close later at high speeds, effectively preventing flutters. Apart from experimental studies, numerous investigations in the literature focus on the numerical analysis of valve movements. Mu et al. [2] developed a model to analyze valve movements at various limiter heights. The numerical analysis demonstrated that, in order to prevent delayed valve closure, the limiting distance should not exceed a certain range. However, it should also not fall below a specific level to avoid an increase in rebound caused by contacting the limiter. While many reciprocating compressors do not utilize limiters on their suction valves, they are present in certain applications. Wang et al. [3] conducted a numerical study on the movement of suction valves with varying limiter heights, revealing that an increase in limiter height leads to delayed closure beyond a certain point. In a separate experimental investigation by Bacak et al. [4], the discharge line losses of hermetic reciprocating compressors were explored under different operating conditions and speeds. The results emphasized the impact of varying operating speeds and pressures on the losses. In the context of this study, P–V diagrams were generated for a hermetic reciprocating compressor used in refrigerators, considering two different limiter heights, two different RPM values, and three different compression ratios. The COP and capacity values were obtained from calorimeter measurements and subsequently compared.

2 Experimental Setup and Procedure

In this study, the effects of different limiter heights on a compressor with a compression volume of 10 cc, commonly used in refrigerators, were examined. Data were obtained by drilling the valve plate from the side and placing a pressure transducer, as depicted in Fig. 1a. High-resolution and high-speed response pressure sensors

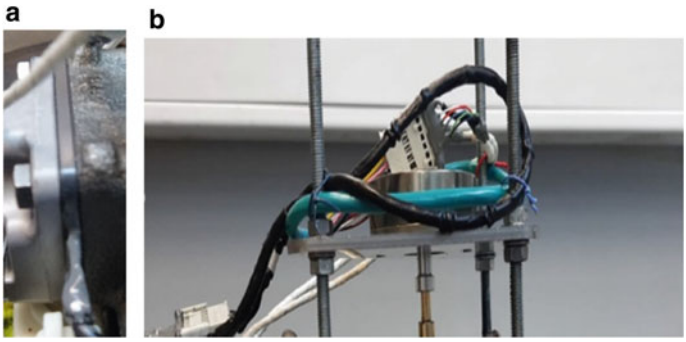


Fig. 1 **a** Valve plate sensor installation, **b** encoder installation

were utilized with a frequency of 50 kHz to ensure clear results at high RPMs. These pressure transducers were capable of measuring within the range of 0–17 bar and producing a 100 mV output voltage, with an accuracy of approximately ± 5 mV. PV diagrams, widely utilized in the literature, play a crucial role in comprehending compressor performance. Real et al. [5] developed a methodology for PV measurement that synchronizes with valve movements and confirmed the accuracy of their results using this approach.

In the present study, cylinder pressure was synchronized with valve displacements using a magnetic encoder with 0.05 degree measurement accuracy, capable of measuring up to 10,000 rpm, as shown in Fig. 1b. Valve displacement measurements were attempted using a strain gauge attached to the discharge valve. However, due to the strain gauge's deformation caused by high pressure, temperature, and vibration, reliable data could only be obtained under conditions of low compression ratio and low rotation speed. This issue will be further discussed and analyzed in detail in the experimental results section.

3 Numerical Model

To further investigate the experimentally obtained results, a 1-D dynamic reciprocating compressor model was employed. The model was developed using the Modelica language and implemented through the Dymola interface. Detailed modeling was achieved by utilizing subcomponents from the commercial TIL Library. The code incorporates thermal and flow models for each subsystem of the compressor, including muffler volumes, a cylinder chamber, and valves. For a visual representation of the model, refer to the schematic provided in Fig. 2, which provides a general overview of the system.

In the left part of Fig. 2, the mufflers are depicted as rectangular shapes. They consist of adiabatic pipes, where pressure drops resulting from frictional effects and

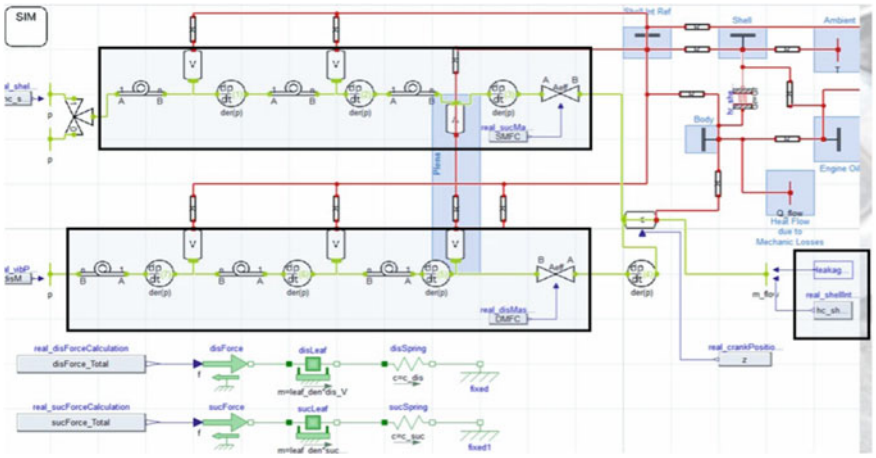


Fig. 2 Schematic of 1D reciprocating compressor model

momentum changes are modeled using flow equations, and volumes that are influenced by thermal models. In the pipes, equations for mass, momentum, and energy balance are solved, while the volumes are modeled based on mass and energy conservation. This decoupling of the momentum equation significantly reduces simulation times while still allowing for modeling pressure oscillations in the plenum volumes of the mufflers. A thermal circuit analogy is implemented for the thermal system in the compressor. Components such as the refrigerant shell, engine oil, cylinder chamber body, and muffler volumes are treated as lumped components, and the appropriate heat coefficients are adjusted based on detailed temperature experiments conducted in real life scenarios. The Woschni heat transfer model [6] is utilized specifically for the heat transfer model inside the cylinder chamber. On the right-hand side of Fig. 2, components responsible for piston leakage calculations are highlighted within a rectangle. These components are added as additional ports to the cylinder chamber volume, in addition to the suction and discharge ports. Through these ports, the refrigerant flows according to the displacement of the piston leaves. In this model, the motion of the valve leaves is represented using a spring-mass-damper system, which is a widely recognized method for valve leaf modeling and has been used in the literature [7, 8]. The governing equation is based on Newton's 2nd Law and can be expressed as follows:

$$m\ddot{x} + d\dot{x} + kx = \sum_i F_i \tag{1}$$

In the equation, m represents the equivalent moving mass of the valve leaf, while d and k correspond to the damping coefficient and spring constant, respectively. These values are found by using experimental methods such as natural frequency inspection for k and logarithmic decrement of the displacement of leaves for d. The logarithmic decrement experimental setup for finding the damping coefficient is

constructed such that a leaf is clapped to a fixture and a laser sensor for displacement measuring is embedded in this fixture. After an initial displacement is introduced, the leaf is released from its configuration, and displacement values are recorded with respect to time. On the right-hand side of the equation, F_i includes the force due to pressure differences between surfaces of the leaf and pressure drag force around the leaf. Forces due to pressure differences between surfaces are calculated as such:

$$F_{pres} = c_f \frac{\pi}{4} D_{leaf}^2 \left(P_{upstream} - P_{downstream}\right) \tag{2}$$

In Eq. 2, c_f stands for force coefficient. While modeling the 3-dimensional geometry of the leaf and its opening movement, one should convert to a 1-dimensional system by getting force coefficients from a 3-dimensional numerical analysis. Design of numerical experiments of 3D Analysis planned in a semi-transient approach. Port hole and displaced leaf are represented in geometry. Steady analyses are conducted for 4 different leaf openings and in those displaced leaf orientations pressure difference as boundary conditions are applied. When the pressures on both faces of the leaf in different displacement orientations are numerically obtained from those 3D analyses, the force due to pressure force is calculated by multiplying by surface areas. The numerically calculated force values are then compared with the theoretical force on valves, considering different pressure differences and leaf displacements, using a 1D geometry. For each displacement configuration, a force coefficient value is determined. By applying linear regression to the four force coefficient points, a continuous function for the force coefficient as a function of displacement is obtained. In the case of discharge leaf, displacement of leaf, x, is restricted by a limiter, reflecting real-life conditions. Therefore, the experimental study of reducing the discharge limiter height is also conducted numerically using this model.

4 Experimental Result

The experimental results are presented in Table 1, which includes the capacity measured under equilibrium conditions for the compressors connected to the calorimeter, as well as the change in COP between the prototypes. Additionally, the change in compression work from Prototype 1 to Prototype 2, obtained from PV diagrams, is included in Table 1. In the first prototype, the limiter height was set to the normal height, while in the second prototype, it was adjusted to be reduced by 1/3 from the normal height. ‘Pc’ indicates condenser pressure. ‘P’ means instantaneous cylinder pressure. The table also includes data that is dimensioned in the form of P/Pc and examined graphically. The term “Cr” refers to the compression ratio, which represents the ratio of the condensing pressure to the evaporating pressure. The change in COP between the prototypes and the change in compression work obtained from PV diagrams from Prototype 1 to Prototype 2 are also provided in Table 1.

Table 1 Experimental results chart

Condition	RPM	Prototype	Capacity (%)	COP (%)	Compression work (%)
Cr = 12	1300	Normal limiter height	100.0	100.0	100.0
		Lower limiter height	102.3	100.8	101.4
	3000	Normal limiter height	100.0	100.0	100.0
		Lower limiter height	99.8	98.1	101.8
Cr = 9	1300	Normal limiter height	100.0	100.0	100.0
		Lower limiter height	100.9	98.8	102.1
	3000	Normal limiter height	100.0	100.0	100.0
		Lower limiter height	97.7	97.4	100.3
Cr = 5	1300	Normal limiter height	100.0	100.0	100.0
		Lower limiter height	99.9	99.5	100.4
	3000	Normal limiter height	100.0	100.0	100.0
		Lower limiter height	99.2	94.5	105.0

Upon examining Table 1, is evident that there is a significant increase in the compression ratio, particularly at high speeds, due to the change in the limiter height. Although the COP values remain close to the results obtained at low speeds for the three examined conditions, the positive effect of the limiter height reduction is observed primarily in the Cr 12 condition, which represents the highest compression ratio.

In the condition with a compression ratio of 12, which is the highest among the experimental studies, the highest-pressure values for Prototype 1 were observed at 1300 rpm, reaching 1.036 at 328 degrees. For Prototype 2, the highest-pressure value was found at 327 degrees with a P/Pc ratio of 1.039, indicating a slight shift of 1 degree compared to Prototype 1. Prototype 1 exhibits a pulsative pressure distribution, while Prototype 2, with the reduced limiter height, shows a smoother pressure distribution in the exhaust stage after the initial overshoot. The experimental results indicate that there was a 1.4% increase in compression work, despite having a less pulsative flow. However, there was an approximate 0.8% improvement in COP, attributed to a 2.3% increase in capacity. It is believed that this improvement in volumetric efficiency is not solely due to thermal effects, but rather the result of improved closing timing of the valves, which work more smoothly due to the improved pressure swing, as shown in Fig. 3a.

In the case of Prototype 1 at 3000 rpm, the maximum pressure observed is 1.120 P/Pc at 332 degrees, while for Prototype 2, it is 1.150 at 333 degrees. It is noteworthy that the overshoot continues to increase for a certain period after the flow begins and then exhibits a slower decrease compared to Prototype 1. The reduction in limiter distance results in a wider pressure release during the exhaust phase, leading to a less pulsating and more stable flow in Prototype 2. However, due to the higher pressures in Prototype 2 compared to Prototype 1, the work spent on compression increases

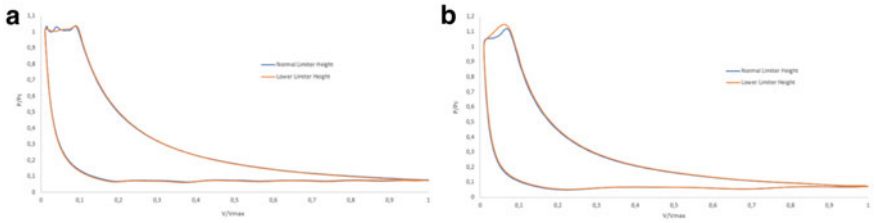


Fig. 3 **a** Cr = 12, 1300 rpm experimental result. **b** Cr = 12, 3000 rpm experimental result

by 1.8%. Although the capacities are similar, this increase in work negatively affects the COP.

At a compression ratio of 9, the peak pressure occurs at 323 degrees for both prototypes at 1300 rpm, shown in Fig. 4a. The first overshoot values are 1.059 for Prototype 1 and 1.081 for Prototype 2. In Prototype 1, there are three different local overshoot values, indicating a less stable pressure distribution. In contrast, Prototype 2 exhibits a more stable pressure distribution. Furthermore, the compression work increased by 2.1%, while there was only a 0.9% increase in capacity.

At high speeds and the same compression ratio, the pressure–volume diagram follows a similar trend to the 3000-rpm test in the first test conditions, shown in Fig. 4b. The maximum pressure value for Prototype 1 is 1.185 at 328 degrees, while for Prototype 2 it is 1.223 at 330 degrees. However, due to the narrow flow area and high flow rate, the high overshoot results in a 2.3% reduction in capacity and an inclination towards increased compression power.

In the post-test condition with a compression ratio of 5, the reduction in flutters is most evident. Due to the low compression ratio, the exhaust phase begins earlier, resulting in a longer exhaust time and more pronounced pressure swings. In the 1300 rpm test, the first overshoot for Prototype 1 occurs at 309 degrees with a value of 1197. The highest overshoot value is observed during the third flutter, reaching 1287. For Prototype 2, the initial overshoot occurs at 310 degrees with a value of 1236. On the other hand, the capacity and compression work values are similar for both prototypes in the post-test condition.

At 3000 rpm, the overshoot for Prototype 1 is 1355 at 318 degrees, and for Prototype 2 it is 1450 at 326 degrees. The pressure continues to increase after the beginning

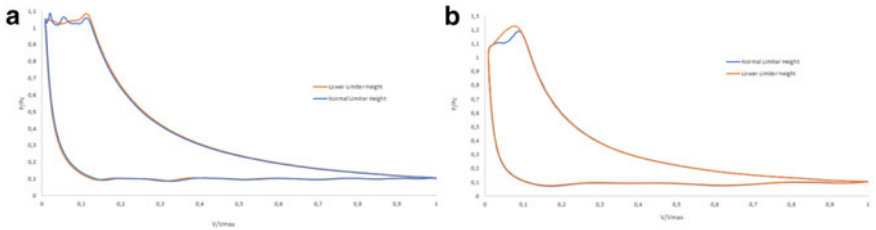


Fig. 4 **a** Cr = 9, 1300 rpm experimental result. **b** Cr = 9, 3000 rpm experimental result

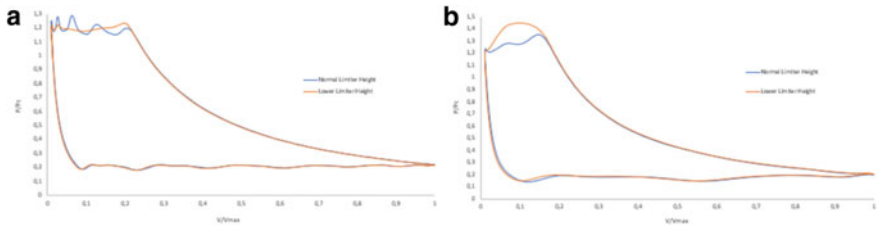


Fig. 5 **a** Cr = 5, 1300 rpm experimental result. **b** Cr = 5, 3000 rpm experimental result

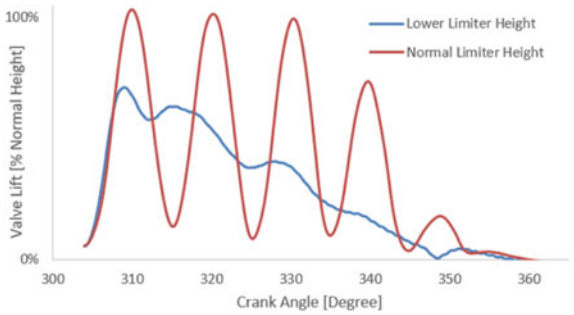


Fig. 6 Compression ratio = 5, 1300 rpm experimental valve lift result

of the exhaust stage for 8 degrees with the decrease in compression ratio. Despite a 0.8% decrease in capacity, there is a significant 5% increase in compression work.

As shown in Fig. 6, in the 3rd test condition with the lowest compression ratio and at 1300 rpm, the exhaust valve displacements were attempted to be measured using strain gauges. Although the data obtained were not reliable at high compression ratios and high rpm, it was observed that the flutter movements in the valve leaves were effectively damped according to the P–V diagram. There was an improvement of approximately 1 degree in the timing of leaf.

5 Numerical Result

In the results obtained using the numerical model, there is a close similarity with the experimental results at low rotation speeds. However, at high speeds, there is a slight deviation between the numerical and experimental results. Figure 7b presents the numerical results for the condition with a compression ratio of 12 and a rotation speed of 3000 rpm, highlighting the differentiation from the experimental results. Table 2 shows the numerical results including the capacity, COP, and compression works. It is observed that the overshoot amounts in the numerical results are higher compared to

the experimental results. Future studies aim to improve the model parameters, especially for high rotational speeds, to better match the experimental data. The current analysis focuses on the modeling results for low speeds. The numerical results demonstrate that the change in compression work is proportional to the compression ratio, consistent with the experimental findings. Furthermore, reducing the limiter distance tends to increase compression work, particularly at higher compression ratios. The experimental and numerical results show a similar trend, with the maximum increase in capacity observed at high compression ratios. The experimental studies indicate that the COP values tend to be close for conditions with compression ratios of 9 and 5 when the limiter distance is reduced. Similarly, the numerical results also demonstrate an increase in COP, albeit on a slightly different scale than the experimental data. However, it is evident from both the experimental and numerical results that reducing the limiter distance at low speeds has a more positive effect on COP for the condition with a high compression ratio of 12 compared to other conditions.

The change in compression work from Prototype 1 to Prototype 2, obtained from the PV diagrams, is also included in Table 2. In Prototype 1, the limiter height was set to the normal height, while in Prototype 2 it was reduced by 1/3 from the normal height, as done in the experimental study.

Figure 7a illustrates the effect of reducing the height of the limiter. Similar to the experimental results, reducing the height of the limiter led to a decrease in the number of flutters at lower rpm and resulted in smoother leaf movement, particularly at the beginning of the discharge process. The increase in pressure observed during

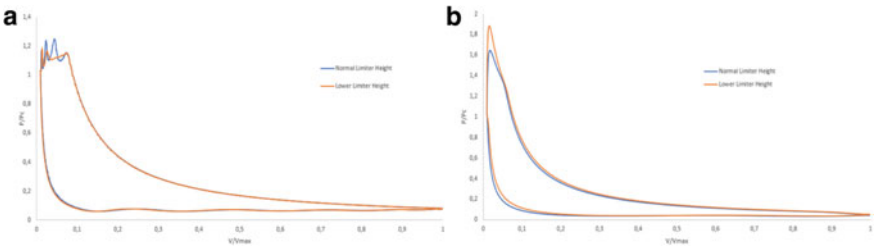


Fig. 7 **a** Cr = 12, 1300 rpm numerical result. **b** Cr = 12, 3000 rpm numerical result

Table 2 Numerical result chart

Condition	RPM	Prototype	Capacity (%)	COP (%)	Compression work (%)
Cr = 12	1300	Normal limiter height	100	100	100
		Lower limiter height	101.1	106.6	105.5
Cr = 9	1300	Normal limiter height	100	100	100
		Lower limiter height	99.7	101.0	98.7
Cr = 5	1300	Normal limiter height	100	100	100
		Lower limiter height	100.1	101.6	98.6

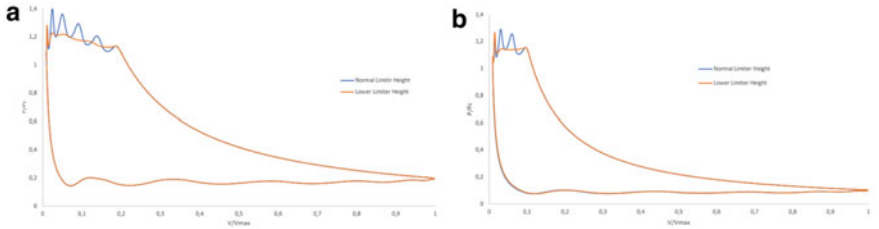


Fig. 8 **a** Cr = 5, 1300 rpm numerical result. **b** Cr = 9, 1300 rpm numerical result

the closing of the valves is closely aligned with the experimental conditions for all tested scenarios.

In the case of lower compression ratio conditions depicted in Fig. 8a and b, flutter movements are more prominent, particularly at low speeds. However, the reduction in flutter movements is evident, indicating improved efficiency. The pressure distribution during the exhaust stage is much smoother, with a significant reduction in flutters. The oscillation of the valve during the closing phase is observed, and its effect on efficiency is noticeable. The oscillation in pressure during valve closure is consistent with the experimental results and has a negative impact on efficiency.

It can be considered that the differentiation between the numerical results and the experimental results, especially at high speeds, falls within the range of numerical approximation. Several factors contribute to this differentiation. Firstly, determining force coefficients is a challenging process, and in this analysis, steady-state flow is assumed with constant valve displacements. Additionally, the thermal model implemented in the numerical model depends on the initial temperature values of the components, which may differ from the time scaling of the flow model. Therefore, starting with temperature values close to steady-state conditions is important. Lastly, the experimentally obtained damping ratio and spring constant do not account for viscous effects around the leaves. These factors may contribute to the differences observed in the height reduction between the numerical model and the experimental results while exhibiting similar characteristics. Nonetheless, it can be argued that the developed numerical model provides valuable insights for experimental research, particularly in the context of lower rotation speeds, falling within an acceptable range of approximation.

6 Conclusion

The results for the effect of the limiter height, which is examined experimentally and numerically, on the compressor efficiency at different compression ratios and speeds are shared. It has been seen in both numerical and experimental results that the prevention of flutter movements by reducing the limiter distance affects the compressor efficiency positively while operating at low speeds under high compression ratio

conditions. However, in experimental studies, a decrease in efficiency is observed at high speeds and low compression ratio conditions. For the reasons mentioned in the numerical results section, although numerically close results cannot be obtained at high speeds, the results are in a similar trend at low speeds. In addition to these parameters, it is thought that improving the effective flow area can contribute to the improvement of efficiency by reducing overshoots by creating less narrowing in the exhaust port section of the flow. By improving the model with the experimental results, it will be tried to get close results for high speeds in future studies.

Acknowledgements The authors would like to thank Arcelik A.Ş. for their support during the experimental research. This study is based on the Master thesis completed at Yıldız Technical University.

References

1. M. Ichihara, A sound reduction solution of rotary compressor by experimental source analysis, in *International Compressor Engineering Conference* (Purdue University, West Lafayette, Indiana, 2022)
2. G. Mu, F. Wang, X. Mi, G. Gao, Dynamic modeling and analysis of compressor reed valve based on movement characteristics. Appl. Therm. Eng. **150**, 522–531 (2019)
3. W. Wu, T. Guo, C. Peng, X. Li, X. Li, Z. Zhang, L. Xu, Z. He, FSI simulation of the suction valve on the piston for reciprocating compressors. Int. J. Refrig. **137**, 14–21 (2022)
4. A. Bacak, A. Pınarbaşı, A.S. Dalkılıç, An experimental study on the determination of a hermetic reciprocating compressor's discharge and suction losses. Proc. Inst. Mech. Eng. Part E: J. Process Mech. Eng. 09544089231154350 (2023)
5. M.A. Real, E.A.G. Pereira, *Using PV Diagram Synchronized with the Valve Functioning to Increase the Efficiency on the Reciprocating Hermetic Compressors* (Purdue University, West Lafayette, Indiana, 2010)
6. G. Woschni, A Universally Applicable Equation for the Instantaneous Heat Transfer Coefficient in the Internal Combustion Engine, SAE Technical Paper 670931 (1967)
7. S.K. Lohn, E.L.L. Pereira, H.F. Camara, D.J. Cesar, Experimental investigation of damping coefficient for compressor reed valves, in *International Compressor Engineering Conference* (Purdue University, West Lafayette, Indiana, 2016)
8. J.L. Gasche, A.D.S.d.L. Dias, D.D. Bueno, J.F. Lacerda, Numerical simulation of a suction valve: comparison between a 3D complete model and a 1D model, in *International Compressor Engineering Conference* (Purdue University, West Lafayette, Indiana, 2016)